Creation mechanism of quantum accelerator modes

P. Ahmadi
Department of Physics, MIT-Harvard Center for Ultracold Atoms, and Research Laboratory of Electronics, Massachusetts Institute of Technology, Cambridge, Massachusetts 02139, USA

G. Behinaein, V. Ramareddy, and G. S. Summy
Department of Physics, Oklahoma State University, Stillwater, Oklahoma 74078-3072, USA
(Received 15 June 2009; published 18 November 2009)

We investigate the creation mechanism of quantum accelerator modes which are attributed to the existence of the stability islands in an underlying pseudoclassical phase space of the quantum delta-kicked accelerator. Quantum accelerator modes can be created by exposing a Bose-Einstein condensate to a pulsed standing light wave. We show that constructive interference between momentum states populated by the pulsed light determines the stability island's existence in the underlying pseudoclassical phase space. We generalize this interference model to incorporate higher-order accelerator modes, showing that they are generated if the rephasing occurs after multiple pulses. The model is extended to predict the momentum structure of the quantum accelerator modes close to higher-order quantum resonances. These predictions are in good agreement with our experimental observations.

DOI: 10.1103/PhysRevA.80.053418 PACS number(s): 37.10.Vz, 05.45.Mt

I. INTRODUCTION

The delta-kicked accelerator has been widely used in studying aspects of the transition to chaos in classical and quantum systems [1]. The experimental study of the quantum delta-kicked accelerator (QDKA) has been possible due to the existence of atom cooling and trapping techniques. Experimentally, the QDKA was realized by exposing a sample of laser-cooled atoms to a pulsed off-resonant standing wave of light in the direction of gravity [2]. The most striking feature of this experiment was the observation of quantum accelerator modes (QAMs) which are characterized by a linear momentum gain with pulse number for a component of the atomic ensemble. The modes appear close to quantum resonance times which are integer multiples of the half-Talbot time [2]. QAMs are important in the fields of quantum chaos [3,4], atomic physics [5,6], and nonlinear dynamics [7]. To more effectively use QAM modes for these studies it is important to understand their creation mechanism.

To this end two theoretical models have been developed to explain the observed behavior of the QDKA and particularly to cast light on the creation mechanism of QAMs. Godun *et al.* [5] developed a theory in which QAMs are created by constructive interference between neighboring momentum states (diffraction orders) populated by the standing-wave potential (phase grating). According to this model, only a few of the momentum states accumulate appropriate relative phases between each kick in order to maintain the condition for constructive interference and give rise to the QAMs. Although this theory's prediction for the average momentum of the QAMs is in excellent agreement with experiments, it was not possible to directly observe the QAM's momentum states structure due to the low-momentum resolution of the experiments utilizing laser-cooled atoms.

In a different approach to understand QAMs, Fishman, Guarneri, and Rebuzzini (FGR) [8] developed a pseudoclassical method to study the QDKA (henceforth referred to as the ϵ-classical model). They showed that a parameter which plays the role of Planck's constant scales with the time deviation from a quantum resonance. Hence, for a time interval between kicks close to a resonance, a classical treatment of the QDKA can provide a good description. Using this approach, they attributed the QAMs to the stability islands that appear in the underlying pseudo-classical phase space of the QDKA. The most celebrated feature of this model was the prediction of higher-order QAMs which was confirmed experimentally shortly thereafter [4]. This was a feature that the interference model was unable to explain.

For experiments on cold atomic samples, the momentum distribution was significantly wider than two recoil momentum and therefore one could not observe the individual momentum states after applying standing waves. This experimental limitation and the fact that the interference model failed to predict higher-order QAMs has played in favor of the ϵ-classical theory such that it has become the theoretical backbone of QDKA research.

The observation of QAMs using a Bose-Einstein condensate (BEC) [9] (see Fig. 1 as an example of the QAM with BEC) has circumvented many of these difficulties. The advantage of using a BEC over laser-cooled atoms is that the BEC's initial state is confined inside a minimum-uncertainty box in the phase space. The very narrow momentum width of a BEC allows us to observe the discreteness of the momentum transferred to the atoms after each kick. These observations reveal that QAMs consist of a limited number of momentum states. Hence we are strongly motivated to revisit the interference model and try to not only generalize it in order to incorporate the higher-order QAMs but also establish a better understanding of the relation between the two theoretical pictures.

The format of this paper is as follows. In Sec. II we briefly review both of the theories. In Sec. II A we lay out the interference model of the QAMs. In Sec. II B we review the ϵ-classical theory followed by Sec. II C where we establish the relation to the interference model. This section ends with the generalization of the interference model to the

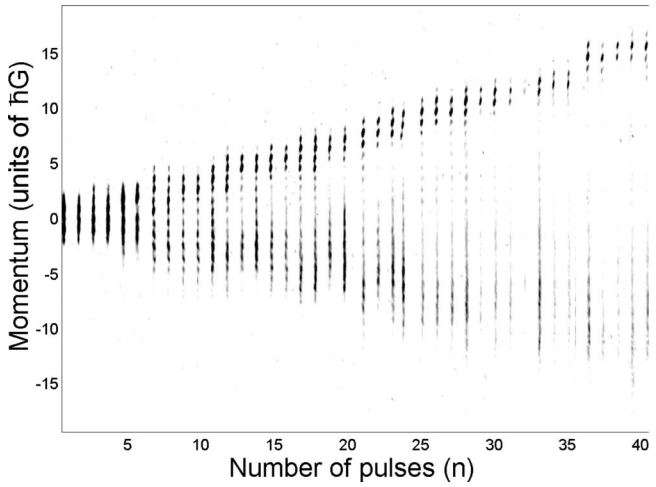

FIG. 1. Experimental data showing the linear momentum gain of an accelerator mode with pulse number. The data shown were created by horizontally stacking 40 time-of-flight images of the condensate, each 8.9 ms after a certain number of kicks (horizontal axis) applied to the BEC. The time interval between the kicks was 72 μs.

higher-order modes. The experimental setup and observations will be presented in Secs. III and IV.

II. THEORY

Both interference and ϵ-classical models are reviewed in this section. Previous theoretical studies [10] have shown that for trapping parameters such as those in our experiment collisional interactions play a minor role in the evolution of QAMs. As such, we do not consider the effect of interatomic interactions in the following analysis. This agrees well with our experimental observations that are well described with theories that do not include any contribution from mean-field effects.

A. Interference model

The following analysis is based on the interference model presented in Ref. [5]. According to this theory the laser-cooled atoms' de Broglie wave packet is assumed to cover many periods of the standing wave. Through the light shift the standing-wave potential can be written as

$$H = \frac{\hat{p}^2}{2m} + mg\hat{z} - \frac{U_{max}}{2}[1+\cos(Gx)]\sum_{N_p}\delta(t-N_pT), \quad (1)$$

with $G=2k$ as the grating vector, k as the light wave vector, m is the atomic mass, and T is the time between pulses. The third term allows this potential to act as a thin phase grating with the net effect being to populate different momentum states according to the following relation:

$$|\psi\rangle = \sum_{n=-\infty}^{\infty} i^n J_n(\phi_d)|p_n\rangle, \quad (2)$$

where J_n is the nth-order Bessel function of the first kind and $\phi_d = U_{max}\Delta t/(2\hbar)$, where Δt is the duration of each now finite pulse. ϕ_d determines the relative populations in the diffraction orders after each pulse is applied. The phase accumulated in the momentum state $|p_q\rangle$, between the N_pth and (N_p+1)th pulse with respect to the phase in the state $|p_0\rangle$ is given by

$$\phi_q - \phi_0 = \frac{\hbar G^2}{2m}Tq^2 + v_iGTq + gGT^2N_pq, \quad (3)$$

where v_i is the initial velocity of atom and q is the total number of grating recoils, $(\hbar G)$ that the atoms have gained up to and including the N_pth pulse. The first term in Eq. (3) is the phase evolution due to the extra momentum q. The second and third terms are the contributions of the initial velocity and the gravitational acceleration to the phase evolution. According to Eq. (3) the phase difference between two *adjacent* momentum states from N_pth pulse to N_p+1th pulse is given by

$$\phi_q - \phi_{q-1} = \frac{\hbar G^2}{2m}T(2q-1) + v_iGT + gGT^2N_p. \quad (4)$$

We now impose the requirement that this phase difference be an integer multiple of 2π for the constructive interference that leads to the creation of a QAM. The above equation can be separated into two parts: one which contains the terms q and N_p (which change with time) and another term which is determined by the initial conditions. Thus,

$$\frac{\hbar G^2}{m}Tq + gGT^2N_p = 2\pi ql, \quad (5)$$

$$v_iGT - \frac{\hbar G^2}{2m}T = 2\pi l', \quad (6)$$

where l and l' are integers. These equations can be rearranged to find $p_i=mv_i$ (the initial momentum) and q (the momentum gained by the atoms participating in the accelerator modes),

$$p_i = \left(\frac{l'}{\alpha} + \frac{1}{2}\right)\hbar G, \quad (7)$$

$$q = \frac{N_p}{\gamma}\frac{\alpha^2}{(l-\alpha)}, \quad (8)$$

where $\gamma=\hbar^2G^3/2\pi m^2g$. The parameter α is defined as $\alpha = T/T_{1/2}$, where $T_{1/2}$ as the half Talbot time, is given by

$$T_{1/2} = \frac{2\pi m}{\hbar G^2}. \quad (9)$$

It can also be seen from Eq. (4) that

$$\phi_{q+1} - \phi_q = \phi_q - \phi_{q-1} + 2\pi\alpha, \quad (10)$$

which implies that only a narrow range of diffraction orders around q can maintain the rephasing condition. This becomes even more profound as α increases.

B. ϵ-classical theory and higher-order modes

In the absence of gravity, the Hamiltonian of Eq. (1) reduces to the delta-kicked rotor (DKR); a planar rotor sub-

jected to external periodic driving pulses. The spacial periodicity of the DKRs Hamiltonian allows one to use Bloch theory which states that the quasimomentum β of an atom subjected to a spatially periodic potential is conserved in time. Here β is the fractional part of the momentum expressed in units of $\hbar G$. The term β-rotor is frequently used to refer to rotor state of a particular quasimomentum.

In the presence of gravity the Hamiltonian of Eq. (1) loses its periodicity and quasimomentum is no longer conserved. In order to reduce the Hamiltonian of Eq. (1) to a DKR form, FGR used a gauge transformation and rewrote Eq. (1) in a freely falling frame. The result was a Hamiltonian which was periodic in space but not in time, once again reducing the dynamics to the β-rotor's dynamics. They defined a small parameter $\epsilon=2\pi(T/T_{1/2}-l)$, where l is an integer, and found that $|\epsilon|$ could be assigned the role of Planck's constant. Therefore, for pulse separations close to resonance times, where $\epsilon\rightarrow 0$, the Hamiltonian is a formal quantization of the following classical maps:

$$\theta_{N_{p+1}} = \theta_{N_p} \pm J_{N_p},$$

$$J_{N_{p+1}} = J_{N_p} + \hat{k}\sin(\theta_{N_{p+1}}) \pm \tau\eta, \tag{11}$$

where $\hat{k}=|\epsilon|\phi_d$, $\tau=2\pi\alpha$, and $\eta=mgT/\hbar G$. The dimensionless θ and J parameters are defined as

$$\theta = Gx \bmod(2\pi),$$

$$J_{N_p} = I_{N_p} + \mathrm{sgn}(\epsilon)[\pi\ell + \tau(\beta + N_p\eta + \eta/2)], \tag{12}$$

where $p/(\hbar G)=I/|\epsilon|+\beta$. The map of Eq. (11) can have period-p fixed points. If these fixed points are stable they will be surrounded by islands of stability. If the atomic wave packet has a sizable overlap with one of these islands, its momentum will grow linearly with the number of kicks according to the relation,

$$q = q_0 - N_p\left(\frac{\eta\tau}{\epsilon} + \frac{2\pi\mathfrak{j}}{\mathfrak{p}\epsilon}\right). \tag{13}$$

These QAMs are classified according to their order $\mathfrak{p}$ and jumping index $\mathfrak{j}$. A fixed point $(\mathfrak{p},\mathfrak{j})$ occurs at $J_0=2\pi\mathfrak{j}/\mathfrak{p}$ and $\theta_0=\theta_i$. Figure 2 depicts phase-space portraits of Eq. (11). A (1,0) stable fixed point occurs at $J_0=0$ in Fig. 2(a) where stable points with indexes (10,1) appears in Fig. 2(b). As can be seen a stability island surrounds these stable fixed points, (a) giving rise to a primary QAM and (b) giving rise to a higher-order QAM.

C. Generalized interference model

In this section we show that the stability of a fixed point in the ϵ-classical theory is equivalent to the constructive interference condition between two neighboring diffraction states in the interference model. We start with Eq. (12) and rewrite it in the following form:

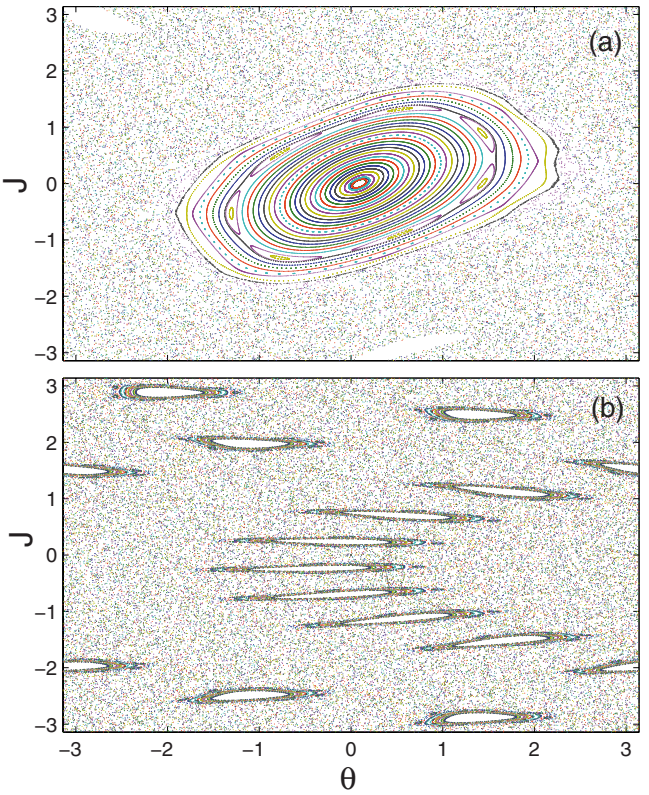

FIG. 2. (Color online) Phase space for the map of Eq. (11) with (a) $\phi_d=1.4$ and $T=29.5$ μs. A stable fixed point with $(\mathfrak{p},\mathfrak{j})=(1,0)$ exists at $J=0$ and $\theta=0.0887$. (b) $\phi_d=1.4$ and $T=66.3$ μs. A stable fixed point with $(\mathfrak{p},\mathfrak{j})=(10,1)$ exists in the cell which gives rise to a higher-order QAM.

$$\frac{J_{N_p}}{|\epsilon|} = \epsilon P + \pi\ell + \tau(\beta + N_p\eta + \eta/2), \tag{14}$$

where P is the integer part of the momentum in units of $\hbar G$ after the N_pth pulse is applied.

As mentioned earlier the $\mathfrak{j}=0$ stable fixed point of this map is at $J=0$ and does not change after applying any number of kicks. By definition, P in Eq. (14) is the total momentum acquired by the fixed point from the pulses. This is equivalent to the definition of q in the interference model allowing us to replace q with P in the following discussion. Also, since β is conserved, its value is determined by the initial velocity via $\beta=mv_i/\hbar G$. Substituting these results and definitions of τ, η, and $\epsilon=\hbar G^2T/m-2\pi l$ into Eq. (14) we have,

$$\frac{\hbar G^2}{2m}T2q - 2\pi ql + \pi l + \left(TGv_i + gGT^2N_p + \frac{1}{2}GgT^2\right) = 0, \tag{15}$$

Where the last term is introduced into the equation because it is written in the freely falling frame. Hence it vanishes in the laboratory frame, with the result that Eq. (15) in the laboratory frame reduces to Eq. (4) up to a constant phase factor of $\pi l-\hbar G^2T/2m$. In other words, the existence of a stable fixed point in the ϵ-classical theory produces the same equation for

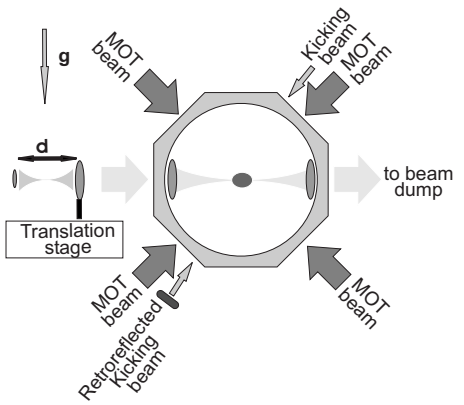

FIG. 3. Schematic of the experiment. The retroreflected kicking beam propagates in 41° relative to the vertical direction. The CO_2 beams was directed into a vacuum chamber in horizontal direction and passed through a 2× beam expander where the second lens was mounted on a translational stage.

the formation of a QAM as the interference theory. Now consider a general (p,j) fixed point with $J_0=2\pi j/p$. Such a point gains $2\pi j/p$ momentum units for each kick, so at the N_pth pulse the total momentum of the fixed point becomes $(2\pi j/p)N_p$. This is npw the right hand side of Eq. (15). Splitting this equation in a similar manner to Eqs. (5) and (6) of the interference model for the time-dependent equation we have

$$\frac{\hbar G^2}{2m}T2q + gGT^2N_p = 2\pi ql + \frac{2\pi j}{p}N_p. \tag{16}$$

Therefore, for a QAM with indexes (p,j) the phase difference between two neighboring momentum states can only be an integer multiple of 2π when $\frac{j}{p}N_p$ is an integer. Hence N_p is an integer multiple of p. This concept can be generalized even more to explain the QAMs at higher-order quantum resonances where $\tau=2\pi(a/b)$ with a and b as positive integer numbers. For QAMs at these resonant times the rephasing happens between momentum diffraction orders that are separated by $b\hbar G$. Hence rewriting Eq. (4) for the momentum states of q and $q-b$ we have

$$\phi_q - \phi_{q-b} = \frac{\hbar G^2}{2m}T(2qb + b^2) + v_iGTb + gGT^2N_pb. \tag{17}$$

Once again separating Eq. (17) into two time dependent and independent parts, the momentum gain of a QAM and the initial condition required for a QAM to exist at higher-order resonances are given by the following:

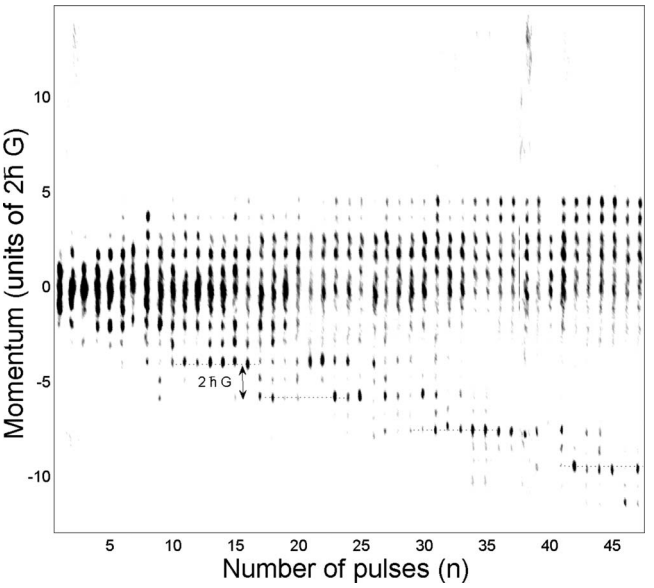

FIG. 4. Experimental data showing the quantum accelerator modes near quarter-Talbot time where the time interval between the kicks was 15.8 μs. The data shown were created by horizontally stacking 47 time-of-flight images of the condensate, each 8.9 ms after a certain number of kicks (horizontal axis) applied to the BEC.

$$q = \frac{N_p}{\gamma}\frac{a^2b}{l' - ab}, \tag{18}$$

$$p_i = \left(\frac{l}{ab} - \frac{1}{2b}\right)\hbar G. \tag{19}$$

III. EXPERIMENTAL SETUP

A schematic of the setup for this experiment is shown in Fig. 3 [11,12]. A standard six-beam magneto-optical trap (MOT) configuration with 24 mW power was used to trap about 50×10^6 atoms. These atoms were then loaded into an optical trap created by focusing a 36 W CO_2 laser beam. Forced evaporative cooling was carried out by reducing the CO_2 laser beam's power in order to created a pure condensate with 45 000 atoms in the $5S_{1/2}F=1$, $m_F=0$ state. The CO_2 laser was then turned off to release the BEC from the optical trap. To make the pulsing standing beam the light used to create the MOT beams was deflected using an acousto-optic modulator into another optical path. This light was 6.7 GHz red detuned from $5S_{1/2}F=1\rightarrow5P_{3/2}F=2$ transition line of the Rb87 and was directed into the chamber at

TABLE I. Theoretical parameters for the interference model for different kicking time intervals. The predicted and observed periodicity of the QAMs with initial momentum are given in the last two columns.

Kicking period	$\alpha\approx$	a/b	b	Δp_i theory	Δp_i observed
Talbot	2	2	1	$\frac{\hbar G}{2}$	$\frac{\hbar G}{2}$
Half-Talbot	1	1	1	$\hbar G$	$\hbar G$
Quarter-Talbot	$\frac{1}{2}$	$\frac{1}{2}$	2	$\hbar G$	$\hbar G$

41° relative to the vertical direction. The momentum distribution was measured by expanding the condensate for a controlled duration, typically 9 ms, and then destructively imaged using an absorptive technique.

IV. EXPERIMENTAL RESULTS

As mentioned earlier the main advantage of using a BEC to realize the QDKA is the improved momentum resolution which allows the observation of the individual momentum states produced by the pulses of the standing wave. Therefore such experiments provide a direct method to examine the validity of the interference model. Figure 1 shows a QAM observed near the Talbot time where the time interval between the kicks was 72 μs. This figure shows that mainly three neighboring momentum states comprise the QAM and almost maintain their population while gaining momentum from the kicks. According to the interference model, these are the momentum states that can rephase at the next kick with a higher momentum. At pulse separations near to the quarter-Talbot time where $b=2$ the rephasing should happen between momentum states with separation of $b\hbar G=2\hbar G$. In other words momentum states with $2\hbar G$ separations should be populated in the QAM. Recently we have been able to observe QAMs near the quarter-Talbot time. Figure 4 shows an example of such data in which the QAM appeared when the time interval between the kicks was 15.8 μs. As is shown by the dotted lines in this figure, the rephasing happens between states with $2\hbar G$ separation, in good agreement with the prediction of the model.

Another aspect of the theory is given by Eq. (19) which indicates a ladder structure for the initial momentum required for observing QAMs. Existence of this structure has been observed with cold atoms [3] and BEC [9] but only for kicking separations close to Talbot and half-Talbot times. According to Eq. (19) this periodicity in the initial momentum depends on the kicking period as $\Delta p_i=\hbar G/ab$. To observe this periodicity a series of data were taken at Talbot, half-Talbot and quarter Talbot times with a constant number of kicks but variable initial momentum. The initial momentum of the condensate was changed by turning off the CO_2 laser and applying the kicking potential after a variable time interval during which the BEC gained momentum under the influence of gravity. Figure 5 shows three data sets taken at (a) $T=15.8$ μs, (b) $T=37.1$ μs, and (c) $T=61$ μs pulse separations for different values of the BEC's initial momentum.

The data in Fig. 5 was created by horizontally stacking 60 time-of-flight images of the condensate, each for a different initial momentum. The theoretical predictions and the observed periodicity of the momentum deduced from Fig. 5 are summarized in Table I which indicates good agreement between the predictions of the model and experiments. The periodicity of the QAMs was deduced from the separation between the QAMs as shown in Fig. 5.

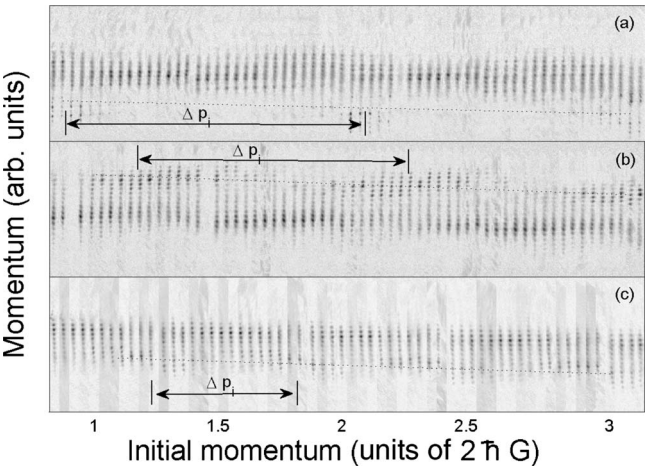

FIG. 5. Experimental data showing the periodicity of quantum accelerator modes with initial momentum. The data were taken after applying 50 kicks with a pulse interval of (a) 15.8 μs, (b) 30 kicks with 37.1 μs, and (c) 10 kicks with 61 μs which are close to near quarter-Talbot, half-Talbot, and Talbot time. The larger number of kicks at the half-Talbot and Talbot time was necessary due to the smaller momentum transfer per pulse.

V. SUMMARY

To summarize, we have generalized the interference model to explain the higher-order QAMs. We have shown that the higher-order accelerator modes are generated by the rephasing of neighboring diffraction momentum states of the matter wave off a standing beam after multiple pulses. Furthermore, the model was extended to the QAMs at higher-order quantum resonances by showing that they are generated by rephasing between momentum states with certain separations set by the quantum resonance time. The relation between this model and the pseudoclassical model was established. This was accomplished by showing that the constructive interference between momentum states populated by the pulsed light determines the stability island's existence in the ϵ-classical phase space. Experimentally, quantum accelerator modes were created by exposing a Bose-Einstein condensate to a pulsed standing light wave. Using this system quantum accelerator modes near quarter-Talbot time were observed. These observations allowed us to validate the interference model and its predictions for the periodicity of the QAMs with initial momentum of the BEC at Talbot, half-Talbot, and quarter-Talbot time.

ACKNOWLEDGMENTS

We would like to thank Ishan Talukdar for helpful assistance in preparing the figures.

[1] Linda E. Reichl, *The Transition to Chaos*, 2nd ed. (Springer, New York, 2004).
[2] M. K. Oberthaler, R. M. Godun, M. B. d'Arcy, G. S. Summy, and K. Burnett, Phys. Rev. Lett. **83**, 4447 (1999).
[3] M. B. d'Arcy, R. M. Godun, D. Cassettari, and G. S. Summy, Phys. Rev. A **67**, 023605 (2003).
[4] S. Schlunk, M. B. d'Arcy, S. A. Gardiner, and G. S. Summy, Phys. Rev. Lett. **90**, 124102 (2003).
[5] R. M. Godun, M. B. d'Arcy, G. S. Summy, and K. Burnett, Phys. Rev. A **62**, 013411 (2001).
[6] R. M. Godun, M. B. d'Arcy, G. S. Summy, and K. Burnet, Contemp. Phys. **42**, 77 (2001).
[7] M. B. d'Arcy, R. M. Godun, G. S. Summy, I. Guarneri, S. Wimberger, S. Fishman, and A. Buchleitner, Phys. Rev. E **69**, 027201 (2004).
[8] S. Fishman, I. Guarneri, and L. Rebuzzini, J. Stat. Phys. **110**, 911 (2003); Phys. Rev. Lett. **89**, 084101 (2002).
[9] G. Behinaein, V. Ramareddy, P. Ahmadi, and G. S. Summy, Phys. Rev. Lett. **97**, 244101 (2006).
[10] L. Rebuzzini, R. Artuso, S. Fishman, and I. Guarneri, Phys. Rev. A **76**, 031603(R) (2007).
[11] P. Ahmadi, G. Behin-Aein, B. P. Timmons, and G. S. Summy, J. Phys. B **39**, 1159 (2006).
[12] P. Ahmadi, B. P. Timmons, and G. S. Summy, Phys. Rev. A **72**, 023411 (2005).